Materials and Design 47 (2013) 372–376

Contents lists available at SciVerse ScienceDirect

Materials and Design

journal homepage: www.elsevier.com/locate/matdes

Short Communication

Effect of stacking fault energy on mechanical behavior of cold-forging Cu and Cu alloys

X.X. Wu, X.Y. San, X.G. Liang, Y.L. Gong, X.K. Zhu *

School of Materials Science and Engineering, Kunming University of Science and Technology, Kunming 650093, China

ARTICLE INFO

Article history:
Received 19 July 2012
Accepted 4 December 2012
Available online 11 December 2012

ABSTRACT

Cu, Cu–2.87 wt% Mn, Cu–4.40 wt% Mn and Cu-10.19 wt% Mn were prepared by cold-forging. The deformation behavior of Cu–Mn alloys is consistent with the Cu-Al alloys and Cu–Zn alloys but without lowering the stacking fault energy to simultaneously increase the strength and ductility. A series of analysis demonstrate that Cu–Mn alloys have a much smaller twin density than low stacking fault energy (SFE) metals, and dislocation strengthening is the major reason for the higher strength. The role of short range order (SRO) in promoting the mechanical properties has also been briefly discussed.

1. Introduction

Stacking fault energy (SFE) is an important material parameter that could affect deformation mechanism during severe plastic deformation (SPD) processing [1–3]. Meanwhile, both a relatively high and low SFE are better for grain refinement in HPT process, since a high SFE has a high rate of recovery while low SFE facilitates more deformation twins [3]. SFE determines the probability of cross slip, which along with dislocation climb is the possible mechanism of dynamic recovery [4]. Researchers have considerable interest in SFE on the bulk ultrafine-grained (UFG,<1 μm) and nanocrystalline (NC,<100 nm) materials which are prepared by a variety of ways, such as high-pressure torsion (HPT) [5], equal channel angular pressing (ECAP) [6], dynamic plastic deformation (DPD) [7], mechanical balling [8], accumulative roll-bonding (ARB) [9] and multiple channel-die compression [10]. With a decrease of SFE by mechanical alloying after ECAP, there is a concurrent increase of strength and ductility in Cu–Al alloys due to the formation of deformation twins and their intersection with dislocation [6]. The previous studies demonstrated the possibility of lowering the stacking fault energy to simultaneously increase the strength and ductility, and there is an optimum stacking fault energy that yields the best ductility [5,11]. The lower SFE also has a higher tendency of twinning compared to the high SFE counterpart, and deformation mechanism can also be transformed from dislocation-dominated to twin-dominated in low SFE Cu alloys [8]. A decreasing SFE leads to better grain refinement, thus further enhancing the strength of the alloys [11]. Manganese is the only element that can be dissolved in copper up to 12% without markedly changing the SFE [12]. Hence, investigation of the deformation behavior of Cu–Mn alloys may yield insight into the influence of alloying elements apart from the (usual) decrease in SFE. We found that the strength and ductility increase simultaneously without SFE decreasing. This result is markedly different from the previous observations. Therefore, it is the purpose of this investigation to study the deformation behavior of cold-forged Cu–Mn alloys without markedly changing the SFE.

2. Experimental procedure

In this work, the starting material was commercially pure copper with a purity of 99.9% and manganese with a purity of 99.7%. Cu, Cu-2.87 wt% Mn, Cu-4.40 wt% Mn and Cu-10.19 wt% Mn were melted in an intermediate frequency furnace. Fig. 1 shows the effect of manganese, aluminum and zinc addition on the SFE value of copper alloys. These as-casts original diameter is 32 mm. Before the forging treatment, the samples were annealed in vacuum at 800 °C for 120 min to obtain homogenous coarse grains. The cast ingots were hot forged to 22 mm in diameter to diminish the effect of mechanical processing and obtain homogeneous microstructures. The samples were sunk in a liquid nitrogen bath after per process of die-forging and the ultimate diameter was 8 mm.

X-ray diffraction (XRD) patterns were acquired on Ricaku D/max 2550 V equipped with a Cu Kα anode (wavelength $\lambda = 1.54$ A). The size of grains and twin density were determined by using an image analyzer [13]. For the Vickers microhardness measurements, each sample was mechanically polished to a smooth surface and then measurements were taken using a HX-1 microhardness tester. Each value is averaged from at least 30 indentations. Tensile tests were performed at room temperature (RT) at a constant strain rate of $1 \times 10^{-4}\ s^{-1}$ by employing a Shimadzu testing machine based on Chines National Standard for the tensile Test (GB-T 228-2002) [14] .

* Corresponding author. Tel.: +86 8715198154; fax: +86 8715161278.
E-mail address: xk_zhu@kmust.edu.cn (X.K. Zhu).

0261-3069/$ - see front matter © 2012 Elsevier Ltd. All rights reserved.
http://dx.doi.org/10.1016/j.matdes.2012.12.006

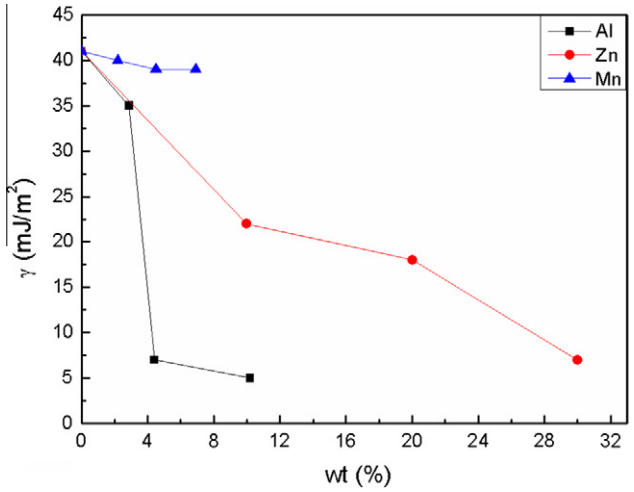

Fig. 1. Variation in SFE values of copper alloys as a function of alloying element concentration.

3. Experiment results

3.1. Microhardness results

The average values of microhardness of each sample are shown in Fig. 2.

As shown in Fig. 2, the microhardnesses of all samples increased with the increasing solid solubility. This is related to solution strengthening due to different amount of Mn contents.

3.2. Tensile test results

Fig. 3a shows the true stress–true strain curves of the Cu, Cu-2.87 wt% Mn, Cu-4.40 wt% Mn and Cu-10.19 wt% Mn alloys at room temperature obtained from the tensile tests. The yield strength and the ultimate strength increase with decreasing stacking fault energy from Cu to Cu-10.19 wt% Mn (increasing Mn content in the alloy without decreasing stacking fault energy). The ductility increased from 0.7% to 1.5% with increased manganese element solubility. The Cu-10.19 wt% Mn alloy has the highest strength and the best ductility. Fig. 3b shows the normalized strain hardening rate against the true plastic strain or the true stress. The normalized work hardening rate θ can be defined as:

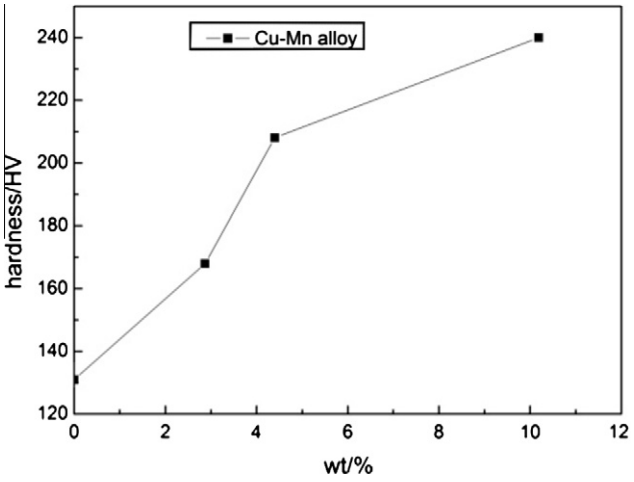

Fig. 2. Microhardness changes of Cu–Mn alloys with the contents of Mn.

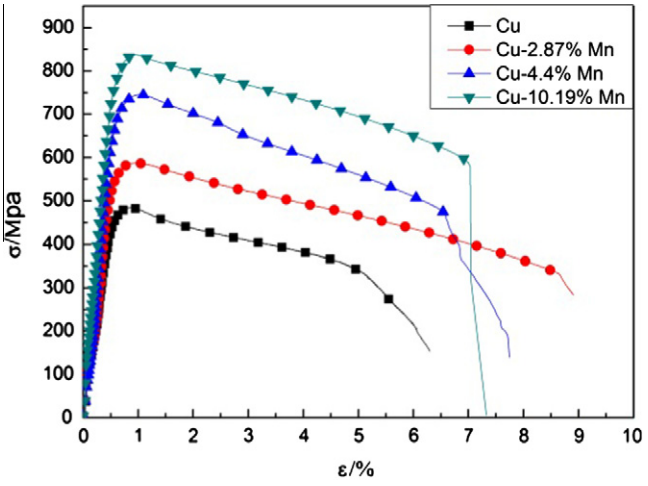

Fig. 3a. True stress–true strain curves of the Cu, Cu-2.87 wt% Mn, Cu-4.40 wt% Mn and Cu-10.19 wt% Mn alloys.

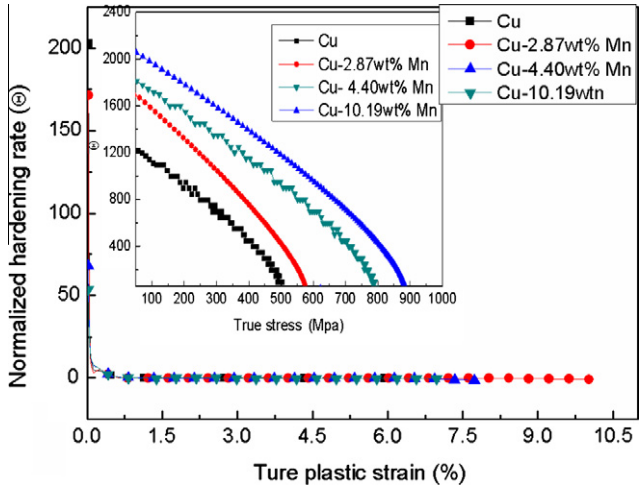

Fig. 3b. The normalized strain hardening rate against the true plastic strain and true stress.

$$\theta = \frac{1}{\sigma}\left(\frac{\partial\sigma}{\partial\varepsilon}\right)\varepsilon \tag{1}$$

where σ and ε are the true stress and the true strain respectively [5]. The normalized strain hardening rate slightly increases with the increasing Mn content. The strain hardening rate corresponds to the changes of ductility.

3.3. XRD results

Fig. 4 demonstrates the XRD patterns of pure copper, Cu- 2.87% Mn, Cu- 4.4% Mn and Cu- 10.19% Mn respectively. The peak shift is mainly due to the increasing Mn content and also the decreased grain size. The dislocation density ρ, may be calculated from the crystallite size d, and microstrain, $\langle\varepsilon^2\rangle^{1/2}$, measured by XRD using the relationship [15]:

$$\rho = \frac{2\sqrt{3}(\varepsilon^2)^{\frac{1}{2}}}{{}^{d}XRD^{b}} \tag{2}$$

where b is the absolute value of the Burgers vector which for FCC metals, is the length of a unit dislocation along the <1 1 0 > direction so that $b = \frac{\sqrt{2}}{2}a$, where a is the lattice parameter.

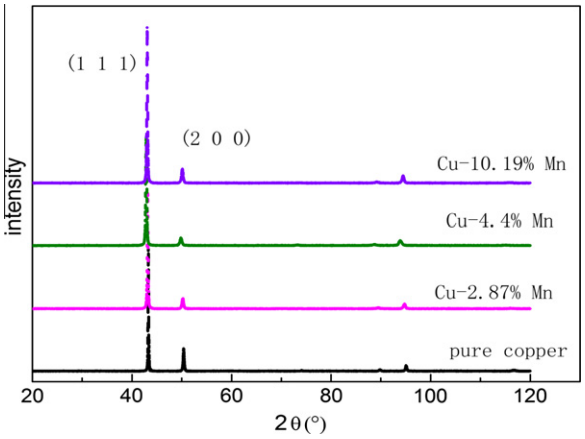

Fig. 4. XRD patterns for pure copper and Cu–Mn alloys.

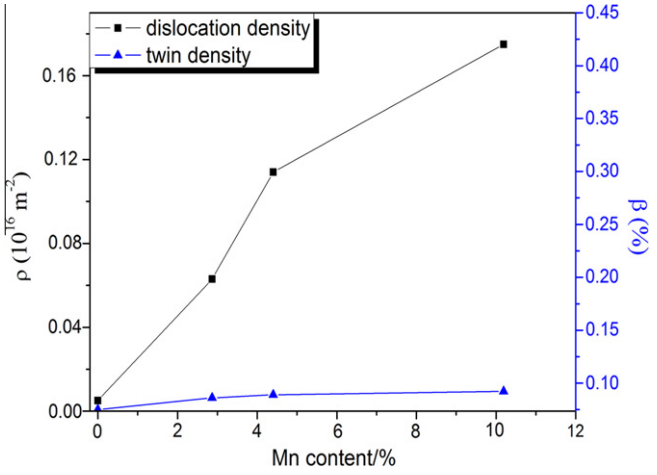

Fig. 5. Changes of dislocation density and twin density with Mn content.

The twin density β, defined as the probability of finding a twin boundary between any two neighboring <1 1 1> planes, was calculated using the expression [16,17]:

$$\beta = \frac{\Delta C \cdot G \cdot (2\theta)_{111} - \Delta C \cdot G \cdot (2\theta)_{200}}{11 \tan\theta_{111} + 14.6 \tan\theta_{200}} \quad (3)$$

where $\Delta C \cdot G \cdot (2\theta)_{111}$ and $\Delta C \cdot G \cdot (2\theta)_{200}$ are the angular deviations of the gravity center from the peak maximum of the <1 1 1> and <2 0 0> XRD peaks, respectively.

The results of dislocation density and twin density are shown in Fig. 5, with the variation of Mn content.

4. Discussion

4.1. The effect of SFE

The yield strength and uniform elongation curves for the Cu alloys for different SFEs are shown in Figs. 6a and 6b, respectively. A series of previous studies demonstrated the possibility of lowering the stacking fault energy to simultaneously increase the strength and ductility [11,18,19], as shown in Figs. 6a and 6b. Surprisingly, we found that the Cu–Mn alloys have the same trend without decreasing SFE. Zhao et al. found that because of its low SFE, the UFG bronze has both higher strength and better ductility than the UFG copper [5]. The higher ductility and strength is derived

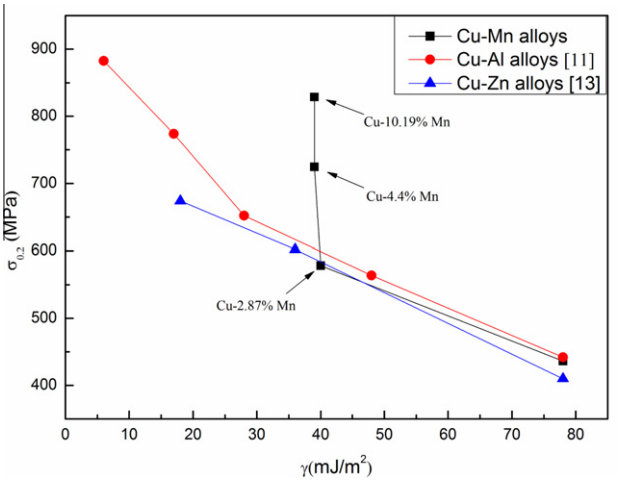

Fig. 6a. The yield strength curves for the Cu alloys for different SFEs.

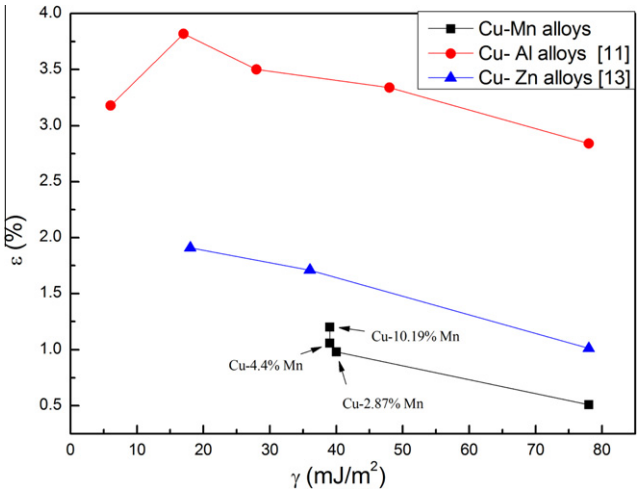

Fig. 6b. Tensile elongation of the Cu alloys as a function of different SFEs.

from its low SFE and high twin density [13]. X-ray diffraction (XRD) data demonstrates that Cu and Cu–Mn alloys have a twin density almost below 0.01%. Twins do play an important role in promoting the strain hardening, which can also help delay the onset of necking, thereby promoting the tensile ductility [20]. The twin density in the Cu–Mn samples obtained from statistical analysis of XRD indicates the twin density did not play a major role in promoting the strain hardening (less than 0.1%). Meanwhile, the manganese addition has a minor effect on the SFE value of copper alloys. SFE is known as an important parameter which can induce the formation of twins and also improve strength by forming more spilt dislocation and stack faults [8,21]; thereby the influence of stacking fault energy on the mechanical properties is negligible. Therefore the twins have no significant impact on the ductility, which means twin strengthening is negligible.

4.2. The effect of dislocation on strength

As can be seen in Fig. 5, the dislocation density increases from 0.005 to 0.175 $\times$ 10^{16} m^{-2} with the increase of Mn content. According to the Taylor Equation, the relationship between the yield strength σ_y and the dislocation density ρ can be described as follows:

$$\sigma_y = \sigma_0 + aMGb\sqrt{\rho} \quad (4)$$

where σ_0 is the friction stress, a is a constant, M is the Taylor factor, and G is the shear modulus [22]. The increasing dislocation density leads to an increase in strength.

4.3. The effect of grain size on strength

The higher strength of the Cu–Mn alloys can also be ascribed to its smaller grain size and solution hardening [23]. Despite of the constant SFE, with increasing Mn content the rolling textures change from the pure metal (copper) type towards the alloys (brass) type, where the rolling textures strongly resembled the results obtained in the Cu–Zn system as a result of a decreasing SFE [12]. Therefore, the texture does not play an important role in this system.

4.4. The effect of short range order (SRO) on ductility

It has been reported that the addition of a certain amount of manganese causes SRO and slip planarity in copper alloys [24,25]. Several previous investigations have reported that a 'glide plane softening' phenomenon associated with short range ordering (SRO) is mainly responsible for planar glide regardless of the value of the SFE in FCC solid solution alloys [25,26]. The contribution of SRO in hindering the total dynamic recovery processes is negligible, while it still triggers slip planarity [26]. Meanwhile, slip planarity is considered to have the same influence in causing a linear hardening effect as deformation twinning, for the reduction of dislocation glide length and dynamic recovery rate [27]. Insufficient ability to strain harden, which was often observed in nanostructured and ultrafine grained metals, leads to the onset of early necking, thus reducing the amount of uniform plastic deformation [18]. Therefore, the SRO obstacles have a contribution to the increased work hardening rate. The higher ductility of the Cu–Mn alloys is derived from its higher Θ, which can be concluded is caused by SRO according to the analysis above. SRO also plays a role in solid solution strengthening [28]. However, more detailed analyses are still needed to further understand the precise role SRO played in Cu–Mn solid solutions.

Special attention should be paid here that unlike the common belief in the deformation mechanism for Cu alloys by severe plastic deformation, where the strength and ductility increase simultaneously with the decrease of SFE [11,29–34], we have increased ductility, or at least retained it without any obvious change of SFE. Therefore we may assume that twinning, induced by a decrease of SFE, may not be the sole mechanism to obtain a good combination of satisfactory strength and ductility.

It is noteworthy that the inhomogeneous microstructure also contributes to the ductility according to the distribution of hardness. The relatively small grains inside can shoulder the ductility in some degree [35].

5. Conclusions

In summary, the SFE plays a minor role in Cu–Mn alloys, the strength of the alloy increases without decreasing SFE and the UE increases simultaneously. The structural investigation of NC Cu–Mn alloys with different Mn contents reveals that the Mn content induced grain size decreasing but dislocation density increasing. The strength of Cu–Mn alloys is due to contributions from solid solution strengthening and defect dislocation strengthening. The higher ductility of the Cu–Mn alloys is derived from its higher working hardening rate, which may be caused by its SRO.

Acknowledgement

The authors acknowledge the financial support from the National Natural Science Foundation of China (NSFC) through the project NSFC-50874056.

References

[1] An XH, Wu SD, Zhang ZF, Figueiredo RB, Gao N, Langdon TG. Evolution of microstructural homogeneity in copper processed by high-pressure torsion. Scripta Mater 2010;63:560–3.
[2] Zhu YT, Liao X. Nanostructured metals: retaining ductility. Nature Mater 2004;3:351–2.
[3] Wu X, Narayan J, Zhu Y. Deformation twin formed by self-thickening, cross-slip mechanism in nanocrystalline Ni. Appl Phys Lett 2008;93:031910–31913.
[4] Sarma VS, Wang J, Jian WW, Kauffmann A, Conrad H, Freudenberger J, et al. Role of stacking fault energy in strengthening due to cryo-deformation of FCC metals. Mater Sci Eng: A 2010;527:7624–30.
[5] Zhao YH, Liao XZ, Horita Z, Langdon TG, Zhu YT. Determining the optimal stacking fault energy for achieving high ductility in ultrafine-grained Cu–Zn alloys. Mater Sci Eng: A 2008;493:123–9.
[6] An X, Han W, Huang C, Zhang P, Yang G, Wu S, et al. High strength and utilizable ductility of bulk ultrafine-grained Cu–Al alloys. Appl Phys Lett 2008;92:201915.
[7] Zhang Y, Tao NR, Lu K. Mechanical properties and rolling behaviors of nano-grained copper with embedded nano-twin bundles. Acta Mater 2008;56:2429–40.
[8] Youssef K, Sakaliyska M, Bahmanpour H, Scattergood R, Koch C. Effect of stacking fault energy on mechanical behavior of bulk nanocrystalline Cu and Cu alloys. Acta Mater 2011;59:5758–64.
[9] Rezaee-Bazzaz A, Ahmadian S, Reihani H. Modeling of microstructure and mechanical behavior of ultra fine grained aluminum produced by accumulative roll-bonding. Mater Des 2011;32:4580–5.
[10] Parimi AK, Robi PS, Dwivedy SK. Severe plastic deformation of copper and Al–Cu alloy using multiple channel-die compression. Mater Des 2011;32:1948–56.
[11] An XH, Lin QY, Wu SD, Zhang ZF, Figueiredo RB, Gao N, et al. The influence of stacking fault energy on the mechanical properties of nanostructured Cu and Cu–Al alloys processed by high-pressure torsion. Scripta Mater 2011;64:954–7.
[12] Engler O. Deformation and texture of copper–manganese alloys. Acta Mater 2000;48:4827–40.
[13] Zhao YH, Horita Z, Langdon TG, Zhu YT. Evolution of defect structures during cold rolling of ultrafine-grained Cu and Cu–Zn alloys: influence of stacking fault energy. Mater Sci Eng: A 2008;474:342–7.
[14] GB-T 228-2002. Metallic materials–Tensile testing at ambient temperature. Beijing: Standard Press of China; 2002.
[15] Zhao YH, Liao XZ, Jin Z, Valiev RZ, Zhu YT. Microstructures and mechanical properties of ultrafine grained 7075 Al alloy processed by ECAP and their evolutions during annealing. Acta Mater 2004;52:4589–99.
[16] Cohen JB, Wagner C. Determination of twin fault probabilities from the diffraction patterns of fcc metals and alloys. J Appl Phys 1962;33:2073–7.
[17] Wagner C. Stacking faults by low-temperature cold work in copper and alpha brass. Acta Metall 1957;5:427–34.
[18] Qu S, An XH, Yang HJ, Huang CX, Yang G, Zang QS, et al. Microstructural evolution and mechanical properties of Cu–Al alloys subjected to equal channel angular pressing. Acta Mater 2009;57:1586–601.
[19] Yang P, Yang H, Tao JM, Li CJ, Shen L, Zhu XK. Influence of stacking fault energy on the mechanical properties and work hardening behavior of Ultra-Fine (UF) grained Cu and Cu alloys. Trans. Tech. Publ.; 2010. p. 1003–8.
[20] Lu L, Zhu T, Shen Y, Dao M, Lu K, Suresh S. Stress relaxation and the structure size-dependence of plastic deformation in nanotwinned copper. Acta Mater 2009;57:5165–73.
[21] San XY, Liang XG, Chen LP, Xia ZL, Zhu XK. Influence of stacking fault energy on the mechanical properties in cold-rolling Cu and Cu–Ge alloys. Mater Sci Eng: A 2011;528:7867–70.
[22] Li YS, Zhang Y, Tao NR, Lu K. Effect of the Zener–Hollomon parameter on the microstructures and mechanical properties of Cu subjected to plastic deformation. Acta Mater 2009;57:761–72.
[23] Zhao Y, Zhu Y, Liao X, Horita Z, Langdon T. Tailoring stacking fault energy for high ductility and high strength in ultrafine grained Cu and its alloy. Appl Phys Lett 2006;89:121906.
[24] Gerold V, Karnthaler H. On the origin of planar slip in fcc alloys. Acta Metall 1989;37:2177–83.
[25] Nortmann A, Neuhäuser H. Deformation behavior of copper based solid solutions at elevated temperatures. Phys Status Solidi (A) 1998;168:87–107.
[26] Hamdi F, Asgari S. Influence of stacking fault energy and short-range ordering on dynamic recovery and work hardening behavior of copper alloys. Scripta Mater 2010;62:693–6.
[27] Hamdi F, Asgari S. Evaluation of the role of deformation twinning in work hardening behavior of face-centered-cubic polycrystals. Metall Mater Trans A 2008;39:294–303.
[28] Dieter GE, Bacon D. Mech Metall. New York: McGraw-Hill; 1986.

[29] Chen X, Lu L. Work hardening of ultrafine-grained copper with nanoscale twins. Scripta Mater 2007;57:133–6.
[30] Lu L, Dao M, Zhu T, Li J. Size dependence of rate-controlling deformation mechanisms in nanotwinned copper. Scripta Mater 2009;60:1062–6.
[31] Tian Y, An X, Wu S, Zhang Z, Figueiredo RB, Gao N, et al. Direct observations of microstructural evolution in a two-phase Cu–Ag alloy processed by high-pressure torsion. Scripta Mater 2010;63:65–8.
[32] Zhu YT, Liao XZ, Wu XL. Deformation twinning in nanocrystalline materials. Prog Mater Sci 2012;57:1–62.
[33] Lu L, You ZS, Lu K. Work hardening of polycrystalline Cu with nanoscale twins. Scripta Mater 2012;66:837–42.
[34] San XY, Liang XG, Cheng LP, Li CJ, Zhu XK. Temperature effect on mechanical properties of Cu and Cu alloys. Mater Des 2012;35:480–3.
[35] Wang Y. CM, Zhou F, Ma E. High tensile ductility in a nanostructured metal. Nature 2002;419:912–5.